



Favorable combination of positive and negative electrode materials with glyme–Li salt complex electrolytes in lithium ion batteries

A. Orita^{a,*}, K. Kamijima^a, M. Yoshida^a, K. Dokko^b, M. Watanabe^b

^a Research & Development Center, Hitachi Chemical Co., Ltd., 13-1 Higashi-cho, 4-chome Hitachi-shi, Ibaraki 317-8555 Japan

^b Department of Chemistry and Biotechnology, Yokohama National University, 79-5 Tokiwadai, Hodogaya-ku, Yokohama 240-8501, Japan

ARTICLE INFO

Article history:

Received 4 November 2010

Received in revised form

16 December 2010

Accepted 17 December 2010

Available online 7 January 2011

Keywords:

Ionic liquid

Lithium batteries

Glyme

Ether

Electrolyte

ABSTRACT

Tetraglyme (G4)–lithium bis(trifluoromethanesulfonyl)amide (TFSA) complexes with different G4 ratio were investigated. An increase in the amount of G4 led to the decrease in the viscosity, and increase in the ionic conductivity of the complex, and G4–LiTFSA showed higher thermal stabilities than the conventional organic electrolyte, when the molar ratio of G4 was more than 40 mol%. The increase in the G4 amount improved the rate capabilities of Li/LiCoO₂ cells in the range where the molar ratio of G4 was between 40 mol% and 60 mol%. The stable Li ion intercalation–deintercalation was not observed in the Li/graphite cell of [Li(G4)][TFSA] (G4: 50 mol%) without additives. However, the additives for forming solid electrolyte interface (SEI) film, such as vinylene carbonate, vinylene carbonate, and 1,3-propane sultone, led to the charge–discharge performance comparable to that of the conventional organic electrolyte. The adoption of Li₄Ti₅O₁₂ and LiFePO₄ led to excellent reversibilities of the Li half cells using [Li(G4)][TFSA], probably because of the favorable operation voltage. In the case of the LiFePO₄/Li₄Ti₅O₁₂ cell, the cell with [Li(G4)][TFSA] showed the better rate capability than that with the conventional organic electrolyte, when the rate was less than 1 CmA, and it is concluded that [Li(G4)][TFSA] can be the candidate as the alternative of organic electrolytes when the most appropriate electrode–active materials are used.

© 2011 Elsevier B.V. All rights reserved.

1. Introduction

Lithium ion batteries are indispensable system in portable electronic device, such as mobile phone and notebook computers, due to the high voltage and high energy density compared with other rechargeable battery systems. Large-scale lithium ion batteries for electric vehicles and electric power storage systems have been investigated to achieve the further technical developments [1,2]. One of the indispensable factors is the flammability of organic electrolyte in the lithium batteries [3].

Ionic liquids (ILs) are non-volatile, non-flammable and highly conductive organic salts whose melting points are lower than 373 K, often lower than the room temperature, and have been extensively studied as the nonflammable electrolyte for lithium ion batteries [4–7]. 1-Ethyl-3-methylimidazolium (EMIm) based ILs combined with various anions and lithium salts are commonly used in lithium ion batteries. However, the stability of EMIm cations are insufficient, maybe caused by the reduction at low potential due to the C–H proton sandwiched between two nitrogen atoms of the imidazolium cation, which does not result in stable solid electrolyte interface [8]. It has been reported that

ILs based on particular anions, such as bis(fluorosulfonyl)amide (FSA) and fluorosulfonyl(trifluoromethylsulfonyl)amide, have the ability to perform the reversible Li intercalation–deintercalation with graphitized carbon negative electrode [9,10]. However, the worse safety properties of ILs of the FSA anions, [EMIm][FSA] and [1-propyl-3-methylpyrrolidinium][FSA] comparing with the conventional organic electrolytes have been reported [11].

The crystallographic structures, thermal properties and electrochemical properties of complexes comprising Li salts and oligoethers, such as crown ethers and glymes, have been also investigated [12–17]. Our group reported that equimolar complexes of glyme and Li salts showed unique properties similar to ILs [18,19]. For example, glyme triglyme (G3) or tetraglyme (G4)–lithium bis(trifluoromethylsulfonyl)amide (LiTFSA) equimolar complexes are liquid under ambient temperature and have low flammability, low volatility, high lithium ion concentration, and a wide window of electrode potential [20].

In this paper, we report the physicochemical properties of G4–LiTFSA complexes with various ratio of G4 to lithium bis(trifluoromethanesulfonyl)amide (TFSA). We chose G4–LiTFSA equimolar complex, on behalf of glyme–LiTFSA complexes, because G4–LiTFSA equimolar complex showed higher ionic conductivity and lower viscosity than those of G3–LiTFSA equimolar complex [19,20]. The electrochemical properties of a graphitized carbon negative electrode in the G4–LiTFSA complexes, and the effect of the

* Corresponding author. Tel.: +81 29 285 1153; fax: +81 29 285 7101.
E-mail address: a-orita@hitachi-chem.co.jp (A. Orita).

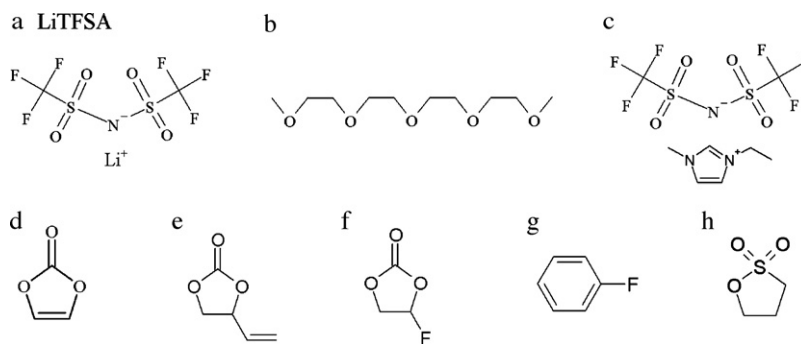


Fig. 1. Chemical structures of tetraglyme (G4), LiTfSA [EMIm][TfSA], and the additives. (a) LiTfSA, (b) tetraglyme (G4), (c) [EMIm][TfSA], (d) vinylene carbonate (VC), (e) vinyl ethylene carbonate (VEC), (f) fluoroethylene carbonate (FEC), (g) fluorobenzene (FB) and (h) 1,3-propane sultone (13PS).

additives, such as vinylene carbonate, into the complexes on the electrochemical properties, and the performances of lithium ion batteries containing G4–LiTfSA as electrolytes and LiCoO₂, LiFePO₄, Li₄Ti₅O₁₂, and graphite as electrode materials were also investigated.

2. Experimental

2.1. Preparation of electrolyte

Chemical structures of tetraglyme (G4), LiTfSA, [EMIm][TfSA], and the additives are shown in Fig. 1. G4 was used after distilling and dehydration with molecular sieves 4A. Typically, G4 and LiTfSA (Kishida Chemical Co., Ltd.) were mixed together in vials and stirred while heating on a hot plate to form homogeneous solutions. When the molar ratio of G4 was 50 mol%, the complex was denoted as [Li(G4)][TfSA]. Vinylene carbonate (VC), vinyl ethylene carbonate (VEC), fluoroethylene carbonate (FEC), fluorobenzene (FB), and 1,3-propane sultone (13PS) were purchased from Kishida Chemical Co., Ltd. and used as the additives to [Li(G4)][TfSA]. The conventional organic electrolyte was 1 M LiPF₆ dissolved in the mixtures of ethylene carbonate (EC), diethyl carbonate (DEC), and dimethyl carbonate (DMC). The volume ratio was 1/1/1 and 1 wt.% of VC was added to 1 M LiPF₆ EC/DEC/DMC.

2.2. Physicochemical properties of electrolytes

The viscosity and ionic conductivity of each electrolyte were estimated by using viscometer (Tokyo Keiki Inc.) and the conductivity meter (CM-201, DKK-TOA Co., Ltd.) with a pair of Pt-black electrodes, respectively. The thermal stabilities of the complexes were investigated by thermogravimetric analysis (Seiko Instrument Inc., TG/DTA6300).

2.3. Electrochemical properties measurements

To prepare the electrode with active layer, we first mixed the ink suspension containing active material, acetylene black, and poly(vinylidene fluoride) (PVDF) solution of N-methyl-2-pyrrolidone. LiFePO₄ and LiCoO₂ were purchased from Hosen Co., Ltd. and used as the active materials. Li₄Ti₅O₁₂ was synthesized by a spray-drying method as follows. The slurry mixture of LiOH, anatase-type TiO₂, PVA, and water dried using a spray-drier. The obtained powder was calcined at 1073 K for 10 h, and Li₄Ti₅O₁₂ was obtained. The graphitized carbon, with an average size particle size of 20 μm and the surface area of 4 m² g⁻¹, was home-made from natural graphite. The average particle sizes of LiFePO₄, LiCoO₂, graphitized carbon, and Li₄Ti₅O₁₂ were 6, 9, 20, and 5 μm, respectively. The acetylene black was purchased from DENKI KAGAKU KOGYO KABUSHIKI GAISHA. We then spread the mixture onto an

aluminum foil (20 μm) or copper foil (40 μm) with blade and evacuated it at 353 K for 3 h after drying for 1 h in air. The obtained electrodes were compressed to increase the packing densities. The electrode densities of LiFePO₄, LiCoO₂, graphite, and Li₄Ti₅O₁₂ were 2.0, 2.5, 1.5, and 2.0 g cm⁻³, respectively. The thickness of an electrode was adjusted to between 30 and 40 μm. The electrode contained 85 wt.% active material, 5 wt.% carbon black, 10 wt.% PVDF, and was cut into circular discs of 9 mm diameter for Li half cells. The positive and negative electrodes were cut into circles of 14 and 15 mm diameter for full cells, and the capacity ratio of negative electrode to positive electrode was adjusted to be 1:1.

The coin-type cells were assembled in a glove box under Ar atmosphere. The cell was constructed by setting a couple of electrodes face to face, with a separator inserted between them. The Celgard #2300 separator was used for the conventional organic electrolyte and the complexes of glyme and LiTfSA. The Celgard #3501 separator was used for the electrolyte based on the ionic liquid, 1 M LiPF₆ [EMIm][TfSA]. To carry out the charge–discharge testing, we used a TOSCAT-3100 charge–discharge system, from Toyo System Co., Ltd. The measurements of the characteristics at the first and second cycles were performed at 0.1 CmA between 3 and 4.2 V, 2.5 and 4.0 V, 0.005 and 1.5 V, 1.2 and 2.5 V, and 0 and 2.8 V for Li/LiCoO₂, Li/LiFePO₄, Li/graphite, Li/Li₄Ti₅O₁₂, and LiFePO₄/Li₄Ti₅O₁₂ cells at 25 °C, respectively. Rate capabilities were measured from 0.1 CmA to 6 CmA at 25 °C. A current of x CmA is 10x mA when the capacity of a cell is 10 mAh. When the different electrolytes were used for the first cycle and second cycle, the cell was disassembled, and the electrode was rinsed by dimethyl carbonate, and the cell was reassembled using the electrode and the pristine coin cell, Li metal, and separator.

We used Solartron SI1287 and SI1260 (Solartron Analytical) to measure of the resistances and the activation energies. AC impedance spectroscopy was measured over a frequency range of 500 kHz to 0.1 Hz with an applied ac voltage of 5 mV. The analysis of resultant Nyquist plots was conducted with Zplot software (Solartron Analytical). It is hypothesized that the semicircle at medium frequency corresponds to the ionic migration process in SEI and the one at lower frequency to the charge-transfer process at the interface between electrolyte and electrode, whereas the intercept at the high frequency end with the real axis represents bulk electrolyte resistance [21,22]. The resistances of ionic migration process in SEI, the charge-transfer process, and bulk electrolyte are denoted as R_{SEI}, R_{CT}, and R_b, respectively. The activation energies of the interfacial lithium ion transfer at graphite in various electrolytes were calculated from the slopes of the Arrhenius plots, 1/R_{CT} = A exp(−E_a/RT) at 0.005 V, between 0 °C and 50 °C. The symbols A, E_a, R, and T denote frequency factor, activation energy, gas constant, and absolute temperature, respectively.

The cyclic voltammetry was carried out at the sweep rate of 0.05 mV s⁻¹ between 0.005 V and 1.5 V (vs. Li/Li⁺) using cell with

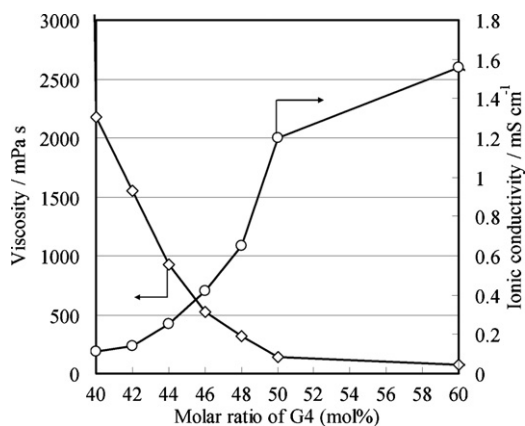


Fig. 2. Viscosities and ionic conductivities as a function of molar ratio of G4 at 25 °C.

three electrodes. The graphitized carbon electrode whose electrode density was 1.0 g cm^{-3} was used as the working electrode, and Li metal as the counter and reference electrode.

3. Results and discussions

3.1. Physicochemical properties of G4–LiTfSA complexes

Fig. 2 shows the viscosities and ionic conductivities of G4–LiTfSA complexes as a function of the molar ratio of G4. The viscosities and ionic conductivities of G4–LiTfSA complexes strongly depended on the ratio of G4 to LiTfSA, and the coordination environment around Li ion might change drastically depending on the molar ratio of G4, as reported in the previous studies [12,23]. When the molar ratio of G4 was less than 50 mol%, the extent of the increase in the viscosity and the decrease in the ionic conductivity was pronounced, inversely depending on the molar ratio of G4. It has been reported that the equimolar mixture of G4 and LiTfSA denoted as $[\text{Li}(\text{G4})][\text{TfSA}]$ showed almost the same self-diffusion coefficients of Li^+ cation and G4 based on the pulse-field gradient spin-echo NMR [18]. Generally, the ionic conductivity is inversely proportional to both viscosity and efficient ionic radius. So, when the molar ratio of G4 is less than 50 mol%, the number of Li ions interacting with one G4 molecule increased, and, the increased number of Li causes the prominent high viscosity and low ionic conductivity of the complexes.

The thermal stabilities of G4–LiTfSA complexes and the conventional organic electrolyte are shown in Fig. 3. In the case of the pure G4, the weight loss started at around 80 °C. The addition of LiTfSA to G4 improved the thermal stability of G4–LiTfSA complexes, suggesting that the thermal stability of G4 depends on the number of Li ions interacting with G4.

3.2. Electrochemical performance of Li/LiCoO₂ cell

Fig. 4 shows the cycle performances of the Li/LiCoO₂ half cells using G4 based electrolytes during the 1st charge–discharge cycle. The molar ratio of G4 had little effect on the Coulomb efficiency of the first cycle. On the other hand, when the molar ratio of G4 was lower than 48 mol%, the discharge capacity decreased. As the obvious decomposition of G4 has not been observed, there might be free glyme molecules in the complexes when the molar ratio of G4 was below 50 mol%. The rapid exchange reaction of G4 molecules in G4–LiTfSA complex with free G4 molecules might inhibit the decomposition. Even when the molar ratio of G4 was less than 50 mol%, all the G4 molecules might be in the state of the pseudo-coordination with Li ions, although the number of Li ion was insufficient in order to form the equimolar complex, $[\text{Li}(\text{G4})][\text{TfSA}]$,

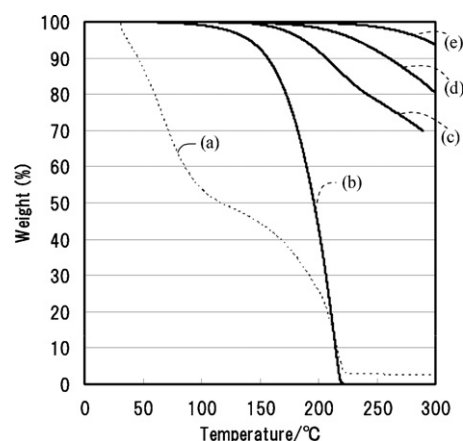


Fig. 3. TG curves of (a) 1 M LiPF_6 EC/DEC/DMC, (b) G4, (c) complex of G4 and LiTfSA (G4: 60 mol%), (d) $[\text{Li}(\text{G4})][\text{TfSA}]$ (complex of G4 and LiTfSA (G4: 50 mol%)) and (e) complex of G4 and LiTfSA (G4: 40 mol%).

when the molar ratio of G4 was less than 50 mol%. The similar result is reported and the results of linear sweep voltammograms and cycle ability of LiCoO_2/Li cell using glyme–Li salts complexes with the different molar ratio showed that the glyme donates lone pairs to the Li^+ cation resulting in the enhancement of oxidative stability of the ether structure [19,20].

The rate capabilities of the Li/LiCoO₂ cells are shown in Fig. 5. The increase in the molar ratio of G4 improved the rate capabilities, however, the discharge capacity drastically decreased over 2 CmA. The rate capabilities of the cells using G4–LiTfSA complexes were inferior to that using the conventional organic electrolyte, 1 M LiPF_6 EC/DEC/DMC + VC. The above-mentioned phenomenon agreed with the previous investigation reported that the diffusion process of Li ion in ionic liquid dominates the limiting current density and the rate capability [24]. The further investigation would be needed for the detail.

3.3. Electrochemical performance of Li/graphite cell

The adaptation of G4–LiTfSA to graphitized carbon negative electrode was investigated. Fig. 6 shows the charge–discharge curves of the Li/graphite cells containing $[\text{Li}(\text{G4})][\text{TfSA}]$ (G4: 50 mol%) and the conventional organic electrolyte. The charge and discharge capacities of the cell with $[\text{Li}(\text{G4})][\text{TfSA}]$ were 376 and 197 mAh g^{-1} , and the reversibility was poor. When Li metal was

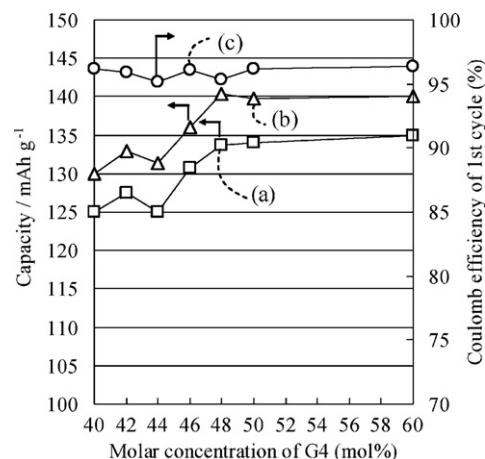


Fig. 4. Charge–discharge characteristics of the Li/LiCoO₂ cells in various electrolytes at the first cycle at 0.1 CmA. (a) Charge capacity, (b) discharge capacity and (c) Coulomb efficiency.

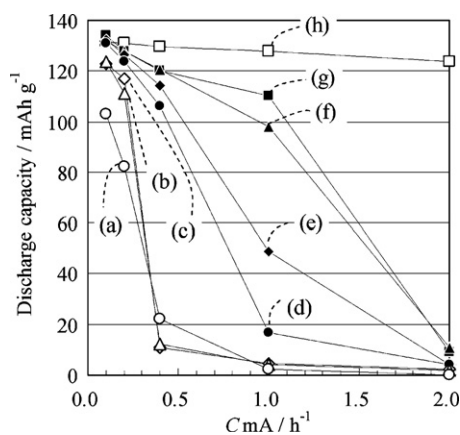


Fig. 5. Rate capabilities of Li/LiCoO₂ cells in various electrolytes. (a) The molar ratio of G4 was 40 mol% in G4–LiTFSA complex, (b) 42 mol%, (c) 44 mol%, (d) 46 mol%, (e) 48 mol%, (f) 50 mol%, (g) 60 mol% and (h) 1 M LiPF₆ EC/DEC/DMC (1/1/1 by volume) + VC1%.

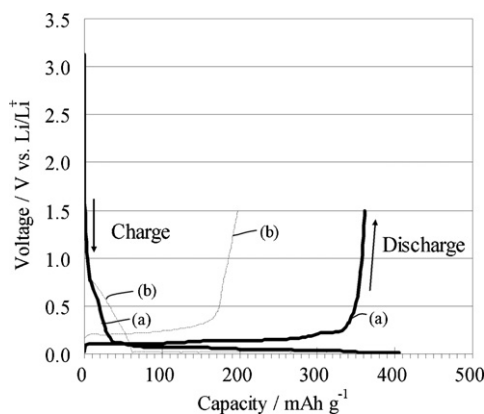


Fig. 6. Charge and discharge curves at the first cycle of the Li/graphite cells. (a) 1 M LiPF₆ EC/DEC/DMC (1/1/1 by volume) + VC1% and (b) [Li(G4)][TFSA] (G4: 50 mol%).

used as the counter electrode, the stable Li deposition–dissolution in [Li(G4)][TFSA] was reported [25]. The poor reversibility of [Li(G4)][TFSA] on graphite negative electrode may be caused by the decomposition of [Li(G4)][TFSA] on the surface of graphite, because the surface of graphite negative electrode is known to be electrochemically active [26]. The similar result was reported that graphite negative electrode does not sufficiently perform in pure ionic liquid electrolyte, excluding ionic liquids based on FSA or fluorosulfonyl(trifluoromethylsulfonyl)amide [9,25,27].

The resistances and activation energies of the interfacial lithium ion transfer were measured in order to examine the key factor for charge–discharge performance of graphite electrode in the different electrolytes, and the result is shown in Table 1. The activation energies for LiPF₆ EC/DEC/DMC (1:1:1 by volume), [Li(G4)][TFSA],

and LiPF₆ [EMIm][TFSA] were 68.7, 66.3, and 88.3 kJ mol⁻¹, respectively. The activation energies of [Li(G4)][TFSA] was similar to that of the conventional organic electrolyte. The value of LiPF₆ EC/DEC/DMC was higher than that observed in the previous work where the activation energy of 58 kJ mol⁻¹ was reported for LiClO₄ EC/DMC (1:1 by volume) with highly oriented prolytic graphite [28,29]. The difference may be explained by that the electrode used in this study contained carbon black and binder polymer, and the sole Li metal was used as both counter and reference electrodes in this study.

The bulk resistance (R_b) of the cell using [Li(G4)][TFSA] at the charged state was 14 Ω cm² which is much higher than that of the conventional cell (0.9 Ω cm²) and 1 M LiPF₆ [EMIm][TFSA] (2.4 Ω cm²). Although the bulk resistance of the cell using [Li(G4)][TFSA] before being charged was 4.0 Ω cm², The bulk resistance of the cell with [Li(G4)][TFSA] was increased by charging process to 14.0 Ω cm², and this result suggests the possibilities of the decomposition of the [Li(G4)][TFSA] at the surface of the graphite negative electrode, the co-intercalation of G4 into the graphite, or the low ability to form SEI on the graphite negative electrode for [Li(G4)][TFSA].

3.4. The effect of forming SEI film on graphite negative electrode

If the low performance of the cell with both [Li(G4)][TFSA] and graphite electrode is attributed to the poor ability of [Li(G4)][TFSA] to form favorable SEI, the cell using [Li(G4)][TFSA] and the graphite electrode with favorable SEI, which is formed by the conventional organic electrolyte, is improved. In particular, we calculated the resistance of the cell whose electrolyte was exchanged from the conventional organic electrolyte to [Li(G4)][TFSA] after one charge–discharge cycle with the conventional one. We also conducted the same experiment using the ionic liquid based electrolyte, 1 M LiPF₆ [EMIm][TFSA], and compared the results of [Li(G4)][TFSA] and 1 M LiPF₆ [EMIm][TFSA].

The result is shown in Table 1. The condition A indicates the conventional condition. In the condition B, we used the cell, which was demolished after charging and discharging in 1 M LiPF₆ EC/DEC/DMC + VC for the first cycle and reassembled using the [Li(G4)][TFSA] for the further cycles. In the condition C, we used the ionic liquid based electrolyte instead of [Li(G4)][TFSA] at the condition B. The R_{SEI} value of the cells using [Li(G4)][TFSA] at the condition B was 90 Ω cm² and almost similar to that of the value of 80 Ω cm² at the condition A. However, the bulk resistance (R_b) and the resistance of ionic migration process in the charge–transfer process (R_{CT}) of the cell using [Li(G4)][TFSA] decreased when the graphite negative electrode with SEI formed in the organic electrolyte was used. The decreases of R_b and R_{CT} might be explained by the suppression of the decomposition of [Li(G4)][TFSA] at the surface of graphite or co-intercalation of G4 into the graphite because the organic electrolyte could form the favorable SEI film for charging and discharging.

Table 1

Resistances and activation energies of the charged Li/graphite cells calculated from the nyquist plots.

Electrolyte condition		Resistance (Ω cm ²)				Activation energy (kJ mol ⁻¹)
		R_b	R_{SEI}	R_{CT}	$R_b + R_{SEI} + R_{CT}$	
1 M LiPF ₆ EC/DEC/DMC+VC	A	0.9	65	50	116	68.7
[Li(G4)][TFSA]	A	14.0	80	400	494	66.3
[Li(G4)][TFSA]	B	5.6	90	50	146	66.0
1 M LiPF ₆ [EMIm][TFSA]	A	2.4	600	1200	1802	88.3
1 M LiPF ₆ [EMIm][TFSA]	C	1.4	600	200	801	81.8

A, conventional condition; B, after charging and discharging in 1 M LiPF₆ EC/DEC/DMC + VC for the first cycle, the cell was disassembled and the electrolyte of the cell was exchanged with [Li(G4)][TFSA]; C, after charging and discharging in 1 M LiPF₆ EC/DEC/DMC + VC for the first cycle, the cell was disassembled and the electrolyte of the cell was exchanged with 1 M LiPF₆ [EMIm][TFSA].

Table 2
Effect of electrolyte at each cycle on discharge and irreversible capacities of Li/graphite cells at first and second cycle.

Electrolyte at 1st cycle	Electrolyte at 2nd cycle	Capacity at 1st cycle (mAh g ⁻¹)		Capacity at 2nd cycle (mAh g ⁻¹)	
		Discharge	Irreversible	Discharge	Irreversible
Carbonate	Carbonate	360	33	360	18
Glyme	Glyme	197	179	190	25
Carbonate	Glyme	359	33	347	67
Ionic liquid	Ionic liquid	23	389	2	30
Carbonate	Ionic liquid	359	35	98	158

Carbonate: 1 M LiPF₆ EC/DEC/DMC+VC; glyme: [Li(G4)][TFSA]; ionic liquid: 1 M LiPF₆ [EMIm][TFSA].

In the case of 1 M LiPF₆ [EMIm][TFSA], R_{SEI} at the condition C is 600 Ω cm² and remained high although we used the electrode with SEI formed in the conventional electrolyte. The similar result has been reported previously [30]. The difference of R_{SEI} between the cells using [Li(G4)][TFSA] and 1 M LiPF₆ [EMIm][TFSA] may be caused by the difference of the electrochemical stabilities between [Li(G4)][TFSA] and 1 M LiPF₆ [EMIm][TFSA], because it is known that [EMIm][TFSA] decomposes at around 0.8 V (vs. Li/Li⁺) without any additives on platinum electrode [31,32].

Table 2 shows the discharge and irreversible capacities of the cells using various electrolytes at the first and second cycles. In the case of the conventional organic electrolyte, the discharge and irreversible capacities were 360 mAh g⁻¹ and 33 mAh g⁻¹ at the first cycle, and 360 mAh g⁻¹ and 20 mAh g⁻¹ at the second cycle, respectively. By contrast, the discharge capacities of the cell using [Li(G4)][TFSA] were 197 mAh g⁻¹ at the first cycle and 190 mAh g⁻¹ at the second cycle. The cell of [Li(G4)][TFSA] whose electrolyte at the first cycle (condition B) was the organic electrolyte showed the high discharge capacity, 347 mAh g⁻¹, although the irreversible capacity was as high as 67 mAh g⁻¹. The high irreversible capacity suggests the remaining of the decomposition of [Li(G4)][TFSA] or co-intercalation of G4 at the graphite negative electrode with SEI, which is formed in 1 M LiPF₆ EC/DEC/DMC+VC. The insufficient suppression of the decomposition of [Li(G4)][TFSA] or co-intercalation of G4 may be explained by the fact that SEI film may be repeatedly destroyed and formed due to the expansion and shrinkage of graphite negative electrode during the intercalation and deintercalation of Li ion at the early stage of the charge and discharge cycles. This reformation of SEI is confirmed by the existence of the irreversible capacity (18 mAh g⁻¹) in the conventional organic electrolyte at the second cycle.

In the case of 1 M LiPF₆ [EMIm][TFSA], the discharge capacity was 98 mAh g⁻¹ when we used the negative electrode with SEI formed in the conventional organic electrolyte (condition C). The low discharge capacity was probably due to the high R_{SEI} value, as shown in Table 1, and lower electrochemical stability of [EMIm][TFSA] than that of [Li(G4)][TFSA].

3.5. The effect of the additives on the performance of graphite negative electrode

In order to improve the charge and discharge characteristics of graphite negative electrode in [Li(G4)][TFSA] without using the electrode with SEI formed in the conventional electrolyte, the effect of the additives for forming SEI film to electrolyte was investigated. VC, VEC, 13PS, FEC, and FB have been used as SEI film-forming agent for lithium ion batteries [33–37]. Fig. 7 shows the cyclic voltammograms (CVs) of G4 and [Li(G4)][TFSA] containing various additives on graphite working electrode using the three-electrode cell.

Fig. 7(a) shows the CVs of G4 without Li salts. The big peak, which is observed between 0 V and 1.5 V in the cathodic scan, corresponds to the decomposition of G4. The decomposition of G4 may be inhibited by the coordination of Li ion as shown by the plot of Fig. 7(b) for [Li(G4)][TFSA]. The oxidative stabilization of G4 by the com-

plexation with Li⁺ was reported from results of the linear sweep voltammograms [19]. The additions of VC and VEC also had the effect for the inhibition of the decomposition of G4 as shown in Fig. 7(c) and (d), but the addition of FB showed little effect as shown in Fig. 7(e).

The charge and discharge characteristics of Li/graphite cells using [G4(Li)][TFSA] with the various additives are shown in Table 3. The addition of VC to [Li(G4)][TFSA] led to the increase in the discharge capacities and the decrease in the irreversible capacities, depending on the amount of VC. When VC was added up to 5 wt.%, the discharge capacity, 359 mAh g⁻¹, is comparable to that of the conventional organic electrolyte, although the irreversible capacity, 64 mAh g⁻¹, was higher than that of the conventional electrolyte. Further improvement may be obtained by increasing the amount of VC. The use of VEC instead of VC decreased the irreversible capacity, probably because the structure of VEC is favorable for the charging and discharging process. In the cases of the use of FEC, 13PS, and FB, the similar improvement was observed, although the extent of the effect on the decreases in the irreversible capacity depends on the kind of the additives. A little effect of FB on the decrease in the irreversible capacity is consistent with the result of the CV, suggesting the decomposition of FB.

Fig. 8 shows the rate capabilities of the Li/graphite cells using [Li(G4)][TFSA] with the various additives. The use of the additives, such as VEC and 13PS, improved the rate capabilities although the capabilities are not sufficient compared to that of the conventional organic electrolyte. The lower rate capabilities of the cell using [Li(G4)][TFSA] than that of the conventional electrolyte are observed in the case of both the Li/LiCoO₂ and Li/graphite cells, and the inferior performance may be caused by the high bulk resistance of [Li(G4)][TFSA].

3.6. The effect of active materials as the positive and negative electrodes

Table 4 shows the charge and discharge characteristic of the Li/Li₄Ti₅O₁₂ cell with [Li(G4)][TFSA]. The charge capacity and the Coulomb efficiency at the first cycle were 159 mAh g⁻¹ and 95.4%,

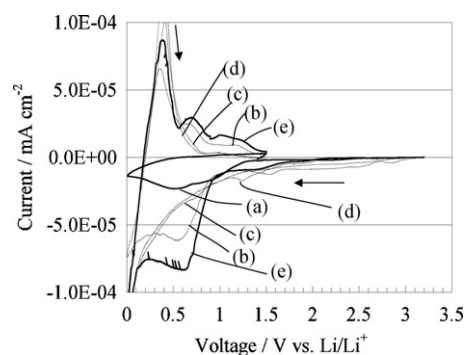
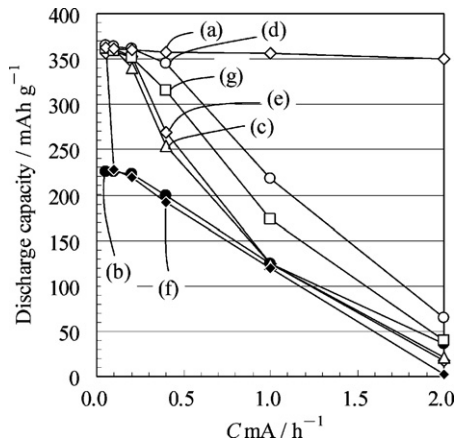
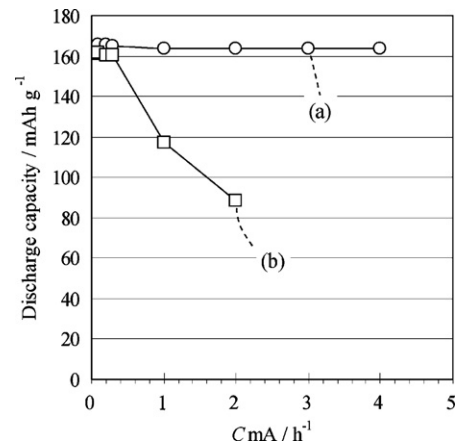


Fig. 7. Cyclic voltammograms of (a) G4, (b) [Li(G4)][TFSA], (c) [Li(G4)][TFSA] + VC5%, (d) [Li(G4)][TFSA] + VEC5% and (e) [Li(G4)][TFSA] + FB5%.

Table 3

Charge–discharge performances of Li/graphite cells using conventional organic electrolyte and [Li(G4)][TFSA] with various additives at the first cycle.

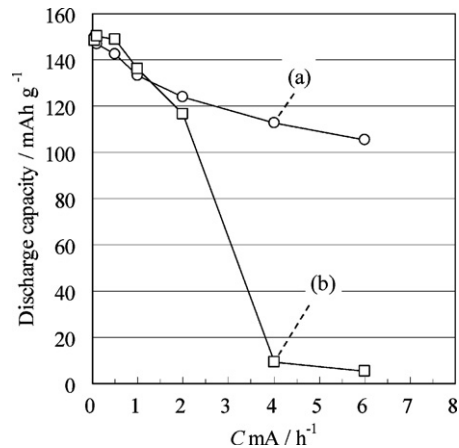
Electrolyte	Additive	Capacity (mAh g ⁻¹)		Coulomb efficiency (%)
		Discharge	Irreversible	
1 M LiPF ₆ EC/DEC/DMC	VC 1%	360	33	91.0
[Li(G4)][TFSA]	0	197	174	53.2
[Li(G4)][TFSA]	VC 1%	280	99	73.8
[Li(G4)][TFSA]	VC 3%	332	81	80.3
[Li(G4)][TFSA]	VC 5%	359	64	84.9
[Li(G4)][TFSA]	VEC 5%	361	42	89.5
[Li(G4)][TFSA]	FEC 1%	329	106	75.6
[Li(G4)][TFSA]	FEC 5%	345	60	85.2
[Li(G4)][TFSA]	FB 1%	329	243	57.5
[Li(G4)][TFSA]	FB 5%	361	82	81.5
[Li(G4)][TFSA]	13PS 5%	364	39	90.3

**Fig. 8.** Rate capabilities of the Li/graphite cells using (a) 1 M LiPF₆ EC/DEC/DMC + VC1% and (b) [Li(G4)][TFSA], (c) [Li(G4)][TFSA] + VC5%, (d) [Li(G4)][TFSA] + VEC5%, (e) [Li(G4)][TFSA] + FEC5%, (f) [Li(G4)][TFSA] + FB5% and (g) [Li(G4)][TFSA] + 13PS5%.**Fig. 9.** Rate capabilities of the Li/Li₄Ti₅O₁₂ cells using (a) 1 M LiPF₆ EC/DEC/DMC + VC1% and (b) [Li(G4)][TFSA].

which are comparable to those of the conventional electrolytes. The high reversibility without any additives may be due to the high operation voltage of Li₄Ti₅O₁₂ (1.55 V vs. Li/Li⁺) and the stable property of [Li(G4)][TFSA] above 1.2 V (vs. Li/Li⁺) [38–40].

The rate capabilities of Li/Li₄Ti₅O₁₂ cell with [Li(G4)][TFSA] and the conventional electrolyte are shown in Fig. 9. The rate capability of Li₄Ti₅O₁₂ in [Li(G4)][TFSA] was comparable with that in the conventional electrolyte at the rate below 0.5 C mA rate. The discharge capacity decreased drastically at the rate more than 1 C mA rate. The decrease may be due to the high viscosity of [Li(G4)][TFSA] and the high bulk resistance of the cell.

The charge–discharge characteristic at the first cycle and the rate capability of the Li/LiFePO₄ cell with [Li(G4)][TFSA] are given in Table 4 and Fig. 10. As shown, the discharge capacity and Coulomb efficiency at the first cycle were 148 mAh g⁻¹ and 96.2%, which were comparable to those using the conventional organic electrolyte. The rate capability was similar to that in the conventional electrolyte at the rate below 2 C mA. However, the discharge capacity of the Li/LiFePO₄ cell with [Li(G4)][TFSA] decreased drastically at the rate

**Fig. 10.** Rate capabilities of the Li/LiFePO₄ cells using (a) 1 M LiPF₆ EC/DEC/DMC + VC1% and (b) [Li(G4)][TFSA].**Table 4**

Charge–discharge performances of Li half cells using various electrode-active materials and electrolytes at the first cycle.

Electrode-active material	Electrolyte	Discharge capacity (mAh g ⁻¹)	Coulomb efficiency (%)
LiCoO ₂	1 M LiPF ₆ EC/DEC/DMC+VC	139	96.1
LiCoO ₂	[Li(G4)][TFSA]	134	96.2
LiFePO ₄	1 M LiPF ₆ EC/DEC/DMC+VC	148	95.9
LiFePO ₄	[Li(G4)][TFSA]	148	96.2
Li ₄ Ti ₅ O ₁₂	1 M LiPF ₆ EC/DEC/DMC+VC	159	95.6
Li ₄ Ti ₅ O ₁₂	[Li(G4)][TFSA]	159	95.4

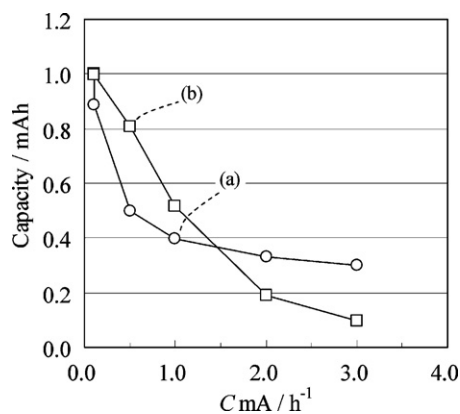


Fig. 11. Rate capabilities of the LiFePO₄/Li₄Ti₅O₁₂ cells using (a) 1 M LiPF₆ EC/DEC/DMC + VC1% and (b) [Li(G4)][TFSA].

of 2 CmA. The reason has not been clarified why the threshold values of the rate capabilities of the Li/Li₄Ti₅O₁₂ cell (0.5 CmA) and Li/LiFePO₄ cell (2 CmA) with [Li(G4)][TFSA] is different.

Fig. 11 shows the discharging performances of the LiFePO₄/Li₄Ti₅O₁₂ cells in the conventional organic electrolyte and [Li(G4)][TFSA]. The significant decrease in the capacities was observed with the increasing discharge current in both electrolytes, probably because of the insufficient improvement of the cell construction. The rate capability of LiFePO₄/Li₄Ti₅O₁₂ cell with [Li(G4)][TFSA] was better than that with the conventional organic electrolyte at the rate less than 1 CmA.

In the results of the Li half cells, the conventional organic electrolyte showed better performance than [Li(G4)][TFSA]. But, in the LiFePO₄/Li₄Ti₅O₁₂ full cell, [Li(G4)][TFSA] showed better performance than the conventional electrolyte. The characteristics of the surfaces of LiFePO₄ and Li₄Ti₅O₁₂ may be improved by adjusting the operation voltage, although the detail of the mechanism has not been clarified. It is concluded that [Li(G4)][TFSA] can be an alternative candidate for current organic electrolytes when the most appropriate electrode-active materials are used.

4. Conclusions

The effect of the molar ratio of G4 in G4–LiTFSA complexes on viscosity, ionic conductivity, and thermal stabilities was investigated. The decrease in the amount of G4 led to the increase in the viscosity, and the decrease in the ionic conductivity, particularly when the molar ratio of G4 was less than 50 mol%. When the molar ratio of G4 was above 40 mol%, G4–LiTFSA showed higher thermal stabilities than the conventional organic electrolyte. The increase in the G4 amount improved the rate capabilities of Li/LiCoO₂ cells in the range of the molar ratio of G4 between 40 mol% and 60 mol%, although all the capabilities of the cells using G4–LiTFSA complexes were inferior to that using the conventional organic electrolyte.

The Li/graphite cell of [Li(G4)][TFSA] (G4: 50 mol%) did not show the stable Li ion intercalation–deintercalation to graphite without the additives. When the graphite negative electrode, on which surface the SEI film was formed using the organic electrolyte in advance, was used, the performance of the Li/graphite cell with [Li(G4)][TFSA] was much improved. The additives for forming SEI film, such as VC, VEC, and 13PS, led to the charge–discharge performance comparable to that of the conventional organic electrolyte, suggesting that the favorable SEI prevents the electrolyte from decomposing on the graphite negative electrode.

The adoption of Li₄Ti₅O₁₂ led to the excellent reversibility of [Li(G4)][TFSA]. The reason may be that the lithium insertion potential of Li₄Ti₅O₁₂ (1.55 V vs. Li/Li⁺) is above the reduction potential of the electrolyte. In the case of the LiFePO₄/Li₄Ti₅O₁₂ cells, the rate capability of [Li(G4)][TFSA] was better than that of the conventional organic electrolyte at the rate less than 1 CmA rate. It is concluded that [Li(G4)][TFSA] can be an alternative candidate for organic electrolytes when the most appropriate electrode-active materials are used.

References

- [1] S. Arico, P.G. Bruce, B. Scrosati, J.M. Tarascon, W.V. Schalkwijk, *Nat. Mater.* 4 (2005) 66.
- [2] K. Zaghbi, P. Charest, A. Guerfi, J. Shim, M. Perrier, K. Striebel, *J. Power Sources* 134 (2004) 24.
- [3] T.H. Nam, E.G. Shim, J.G. Kim, H.S. Kim, S.I. Moon, *J. Electrochem. Soc.* 154 (2007) 957.
- [4] J.S. Wilkes, M.J. Zaworotko, *J. Chem. Soc. Chem. Commun.* 965 (1992) 2.
- [5] M.M. Islam, M.T. Alam, T. Okajima, T. Ohsaka, *J. Phys. Chem. C* 113 (2009) 3386.
- [6] Y.-J. Kim, Y. Matsuzawa, S. Ozaki, K.C. Park, C. Kim, M. Endo, H. Yoshida, G. Masuda, T. Sato, M.S. Dresselhaus, *J. Electrochem. Soc.* 152 (2005) A710.
- [7] A. Paul, P.K. Mandal, A. Samanta, *Chem. Phys. Lett.* 402 (2005) 375.
- [8] P. Bonhôte, A.-P. Dias, N. Papageorgiou, K. Kalyanasundaram, M. Grätzel, *Inorg. Chem.* 35 (1996) 1168.
- [9] M. Ishikawa, T. Sugimoto, M. Kikuta, E. Ishiko, M. Kono, *J. Power Sources* 162 (2006) 658.
- [10] H. Matsumoto, N. Terasawa, T. Umecky, S. Tsuzuki, H. Sakaebe, K. Asaka, K. Tatsumi, *Chem. Lett.* 37 (2008) 1020.
- [11] Y. Wang, K. Zaghbi, A. Guerfi, F.F.C. Bazito, R.M. Torresi, J.R. Dahn, *Electrochim. Acta* 52 (2007) 6346.
- [12] W.A. Henderson, *J. Phys. Chem. B* 110 (2006) 13177.
- [13] W.A. Henderson, N.R. Brooks, W.W. Brennessel, V.G. Young Jr, *Chem. Mater.* 15 (2003) 4679.
- [14] W.A. Henderson, N.R. Brooks, V.G. Young Jr, *Chem. Mater.* 15 (2003) 4685.
- [15] W.A. Henderson, *Macromolecules* 40 (2007) 4963.
- [16] C. Zhang, S.J. Lilley, D. Ainsworth, E. Staunton, Y.G. Andreev, A.M.Z. Slawin, P.G. Bruce, *Chem. Mater.* 20 (2008) 4039.
- [17] C. Zhang, D. Ainsworth, Y.G. Andreev, P.G. Bruce, *J. Am. Chem. Soc.* 129 (2007) 8701.
- [18] T. Tamura, T. Hachida, K. Yoshida, N. Tachikawa, K. Dokko, M. Watanabe, *J. Power Sources* 195 (2010) 6095.
- [19] T. Tamura, K. Yoshida, T. Hachida, M. Tsuchiya, M. Nakamura, Y. Kazue, N. Tachikawa, K. Dokko, M. Watanabe, *Chem. Lett.* 39 (2010) 753.
- [20] M. Nakamura, Y. Kazue, S. Seki, K. Dokko, M. Watanabe, Presented at the 214th ECS Meeting, Honolulu, HI, 2008, p. 742.
- [21] D. Aurbach, M.D. Levi, *J. Phys. Chem. B* 101 (1997) 4630.
- [22] S.I. Yuasa, J. Otsuji, A. Funabiki, M. Inaba, Z. Ogumi, *J. Electrochem. Soc.* 145 (1998) 172.
- [23] J.-C.L.J. Grondin, D. Talaga, *Phys. Chem. Chem. Phys.* 8 (2006) 5629.
- [24] N. Tachikawa, J.-W. Park, K. Yoshida, T. Tamura, K. Dokko, M. Watanabe, *Electrochemistry* 78 (2010) 349.
- [25] T.M. Pappenfus, W.A. Henderson, B.B. Owens, K.R. Mann, W.H. Smyrl, *J. Electrochem. Soc.* 151 (2004) A209.
- [26] K. Xu, *Chem. Rev.* 104 (2004) 4303.
- [27] R.T. Carlin, J. Fuller, W.K. Kuhn, J. Lysaght, P.C. Trulove, *J. Appl. Electrochem.* 26 (1996) 1147.
- [28] T. Abe, H. Fukuda, Y. Iriyama, Z. Ogumi, *J. Electrochem. Soc.* 151 (2004) A1120.
- [29] Y. Yamada, Y. Iriyama, T. Abe, Z. Ogumi, *Langmuir* 25 (2009) 12766.
- [30] H. Zheng, B. Li, Y. Fu, T. Abe, Z. Ogumi, *Electrochim. Acta* 52 (2006) 1556.
- [31] M. Holzzapfel, C. Jost, P. Novák, *Chem. Commun.* (2004) 2098.
- [32] M. Ue, M. Takeda, *J. Korean Electrochem. Soc.* 5 (2002) 192.
- [33] P. Biensan, J.M. Bodet, F. Pertont, M. Brousseau, C. Jehoulet, S. Barousseau, S. Herreyre, B. Simon, Extended Abstracts of The 10th International Meeting on Lithium Batteries, Como, Italy, 2000.
- [34] Y.S. Hu, W.H. Kong, H. Li, X.J. Huang, L.Q. Chen, *Electrochem. Commun.* 6 (2004) 126.
- [35] Z. Xiaoxi, X. Mengqing, L. Weishan, S. Dagen, L. Jiansheng, *Electrochem. Solid-State Lett.* 9 (2006) A196.
- [36] R. McMillan, H. Slegel, Z.X. Shu, W. Wang, *J. Power Sources* 81–82 (1999) 20.
- [37] H. Kita, H. Yumiba, M. Higashiguchi, K. Matsumoto, *JP Patent*, JP 3,748,843 (1998).
- [38] T. Ohzuku, A. Ueda, N. Yamamoto, *J. Electrochem. Soc.* 142 (1995) 1431.
- [39] K.M. Colbow, J.R. Dahn, R.R. Haering, *J. Power Sources* 26 (1989) 397.
- [40] E. Ferg, R.J. Gummov, A. de Kock, M.M. Thacheray, *J. Electrochem. Soc.* 141 (1994) L147.